ACS Medicinal Chemistry Letters

pubs.acs.org/acsmedchemlett
Letter

Synthesis and In Vivo Profiling of Desymmetrized Antimalarial Trioxolanes with Diverse Carbamate Side Chains

Matthew T. Klope, Juan A. Tapia Cardona, Jun Chen, Ryan L. Gonciarz, Ke Cheng, Priyadarshini Jaishankar, Julie Kim, Jenny Legac, Philip J. Rosenthal, and Adam R. Renslo*

Cite This: ACS Med. Chem. Lett. 2024, 15, 1764−1770
Read Online
ACCESS | Metrics & More | Article Recommendations | Supporting Information

ABSTRACT: The recent withdrawal of artefenomel from clinical development leaves no endoperoxide-class agents in the antimalarial pipeline. Synthetic endoperoxides with a desymmetrized structure have demonstrated promising physiochemical and *in vivo* properties. Here we expand on our initial investigation of *trans*-3″ carbamate substitution with a diverse array of amine-, alcohol-, and sulfinyl-terminated analogues prepared in (*S,S*) and (*R,R*) configurations. In general, this chemotype combines low-nM antiplasmodial activity with excellent aqueous solubility but widely varying human liver microsome (HLM) stability. We evaluated 20 novel analogues in the *P. berghei* mouse malaria model, identifying new analogues such as RLA-4767 (**9a**) and RLA-5489 (**9d**), with HLM stability and pharmacokinetic profiles superior to analogues from our initial report (e.g., RLA-4776, **8a**). These new leads approach or equal the efficacy of artefenomel after two daily oral doses of 10 mg/kg, thus revealing a promising chemotype with the potential to deliver development candidates.

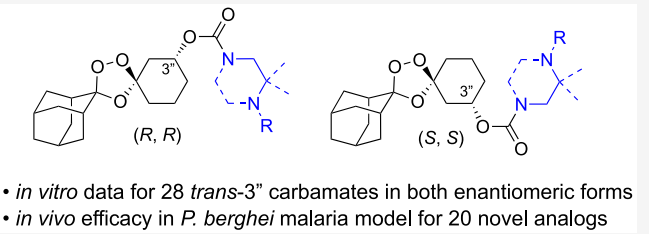

KEYWORDS: *Antimalarials, endoperoxides, trioxolanes, lead optimization, stereoselective synthesis*

Despite notable progress in the preclinical arena, malaria remains a cause of significant mortality, particularly in sub-Saharan Africa.[1] Artemisinin-based combination therapy, the standard treatment for uncomplicated malaria, and intravenous artesunate, the standard for severe malaria, are threatened by the increasing prevalence of artemisinin partial resistance (ART-R), which has recently emerged in eastern Africa.[2,3] Among synthetic endoperoxide-class agents evaluated over the past two decades,[4] the adamantyl-1,2,4-trioxolane pharmacophore identified by Vennerstrom and co-workers[5,6] has produced the only clinical candidates: arterolane (OZ277)[7] which is approved as combination therapy in certain regions, and artefenomel (OZ439),[8] which exhibits a superior exposure profile and predicted efficacy in ART-R (Figure 1).[9,10] Arterolane, used in combination with piperaquine in some countries, has theoretical efficacy concerns, and has had rather limited clinical impact.[11] The long clinical development of artefenomel was recently discontinued, after failing to reach clinical pharmacokinetic and pharmacodynamic benchmarks developed around an admirable, if challenging,[12] goal of achieving single-exposure efficacy. As well, food effects,[13] and complex solution-phase behavior[14] produced formulation challenges that contributed to a difficult clinical path for artefenomel. Accordingly, there are currently no endoperoxide agents in the clinical pipeline.

Herein we report the further evaluation of desymmetrized trioxolane analogues related to arterolane but based on *trans*-3″ substitution with heteroaliphatic carbamate side chains

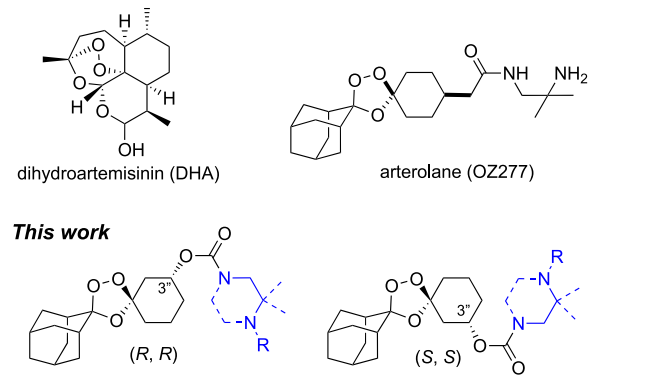

Figure 1. Structure of dihydroartemisinin, arterolane, and the closely related *trans*-3″ carbamate chemotype explored herein and in our preliminary report.[15]

Received: July 25, 2024
Revised: August 29, 2024
Accepted: August 29, 2024
Published: September 5, 2024

(Figure 1). We hypothesized that 3″ substitution with *trans* stereochemistry should offer similarly stability of the endoperoxide bridge as with traditional *cis*-4″ substitution found in arterolane and artefenomel (Figure 2). Indeed, in our

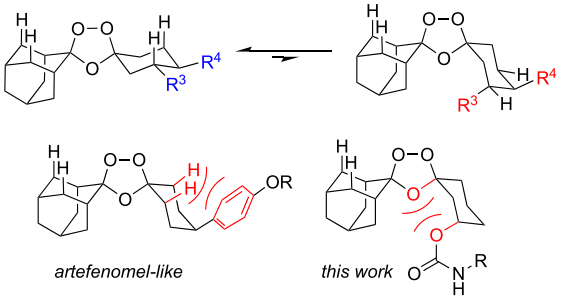

Figure 2. Conformational dynamics of trioxolane antimalarials determine their antiplasmodial effects, with the minor, peroxide-exposed conformer (top right) undergoing Fenton-like reactivity with ferrous iron sources in the parasite, leading to a pharmacodynamic effect. Shown at bottom are the 1,3-diaxial interactions that disfavor the iron-reactive conformer in artefenomel (left) and in the *trans*-R^3 carbamate chemotype explored herein (right).

prior studies, we showed that *trans*-3″ regioisomers of arterolane[16] and artefenomel[17] exhibited similar low-nM antiplasmodial activity and promising in vivo efficacy in the *P. berghei* model of malaria. A move from amide to carbamate side chains produced analogues that were considerably more efficacious than arterolane.[15] Subsequently, O'Neill and co-workers described[18] desymmetrized analogues of the tetraoxane E209 with enhanced solubilities, further supporting this approach toward identifying molecules with differentiated properties. We now expand on our initial survey of this chemotype, describing more than 40 new analogues prepared in enantiopure forms and evaluated in key in vitro ADME and in vivo PK/PD studies.

We aimed to expand on our initial study of *trans*-3″ carbamates, exploring both enantiomeric forms for all new analogues, and preparing (*S,S*) forms of those analogues previously prepared only in the (*R,R*) forms.[15] Thus, (*S,S*)-*trans*-3″ analogues were synthesized in an enantiocontrolled fashion, starting with (*R*)-Taniaphos-mediated asymmetric borylation of cyclohexenone to prepare intermediate **2** bearing the *S* configuration (Scheme 1). Oxidation of the C−B bond and protection of the resulting alcohol as a *tert*-butyldiphenylsilyl (TBDPS) ether afforded ketone **4**. This material undergoes diastereocontrolled Griesbaum co-ozonolysis with adamantan-2-one *O*-methyloxime, to afford the desired *trans* intermediate **5** in a 12:1 diastereomeric ratio (dr) as determined by ^{1}H NMR analysis. Subsequent deprotection of **5** and conversion to the *p*-nitrophenylcarbonate **7** allowed for late-stage diversification into the desired (*S,S*)-*trans*-3″-carbamate analogues **9a-dd**. An analogous approach, but using the antipode of the Taniaphos ligand, was used to prepare (*R,R*)-*trans*-3″-carbamates **8a-dd**.

In our preliminary report,[15] carbamate analogues **8a**, **8b**, **8c**, **8d**, and **8i** were all found to be more efficacious than the arterolane control when administered as a once daily 2 mg/kg oral dose for 4 days (Chart 1). With a single higher dose of 40 mg/kg, analogues such as **8c**, **8j**, **8k**, and **8n** cured 20−60% of animals at day 30, as compared to 100% cures for single-dose artefenomel at this dosage. Importantly, all of the carbamate analogues evaluated showed good aqueous solubility, and many (e.g., **8a**/**b**, **9a**/**b**, **9c**) exhibited excellent stability in human liver microsome (HLM) preparations. From this auspicious starting point, we sought to explore a more diverse array of carbamate side chains and to evaluate all of the analogues in both enantiomeric forms (Chart 1).

Since only three analogues with (*S, S*) stereochemistry had been prepared in our initial study, we began by synthesizing the (*S, S*) forms of previously reported (*R, R*) analogues and evaluating these compounds for their antiplasmodial effects against W2 strain *P. falciparum* (Chart 1, **9d−n**). Similar to the (*R, R*) forms **8d−n**, the (*S, S*) stereoisomers demonstrated potent antiplasmodial effect, with EC_{50} values of the enantiomer pairs generally within 2-fold of each other. Noting the potent antiparasitic effect and favorable solubility of analogues bearing terminal primary amines, we next explored additional (*R, R*) and (*S, S*) analogues bearing 2-substituted ethylenediamine substitutions (**8o−8r**, **9o−9r**) and found that these analogues as well retained potent, low-nM antiparasitic activity. Replacing the terminal amino function with hydroxyl, as in the change from aminooxetanes **8r**/**9r** to hydroxyoxetanes **8s** and **9s** resulted in a ∼ 10-fold decrease in potency, suggesting a role for basic amines in promoting cellular uptake or retention, although the potent morpholine analogues **8f** and **9f** proved an exception to the wider trend.

Scheme 1. Representative Enantiocontrolled Synthesis of (*R,R*)-*trans*-3″ Analogues 9a−dd

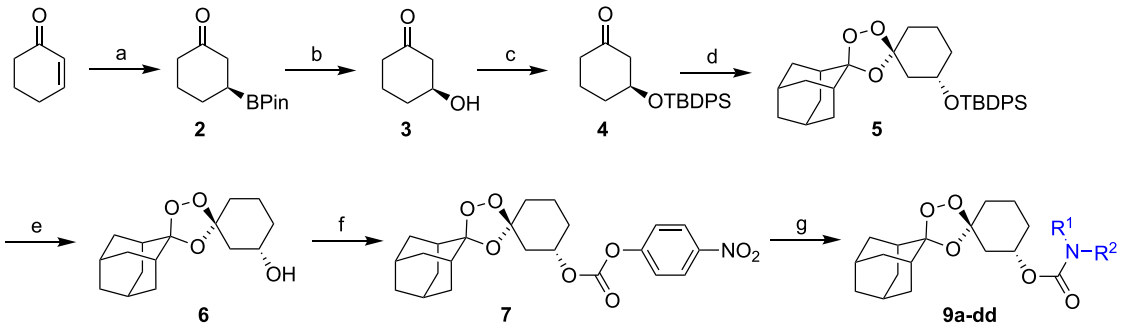

Reagents and conditions: (a) B_2pin_2, t-BuONa, CuCl. (*R*)-Taniaphos, MeOH rt 24 h (b) $NaBO_3{\cdot}4H_2O$, THF/H_2O (3:1) rt 2.5 h (c) t-$BuPh_2SiCl$, imidazole, THF 0 °C to rt 16.5 h (d) adamantan-2-one *O*-methyloxime, O_3, CCl_4 0 °C 3.5 h (e) TBAF, THF 0 °C to rt 3 h (f) 4-$NO_2PhOC(O)Cl$, i-Pr_2EtN, DMAP, CH_2Cl_2 0 °C to rt 18.5 h (g) $R^1(R^2)NH$, Et_3N, CH_2Cl_2. An analogous route was used to prepare analogues (*R,R*)-*trans*-3″ analogues **8a−dd**, using (*S*)-Taniaphos in the first step.

https://doi.org/10.1021/acsmedchemlett.4c00365
ACS Med. Chem. Lett. 2024, 15, 1764−1770

Chart 1. In Vitro Activity of 8a-8dd and 9a-9dd against *P. falciparum* (EC_{50} ± SEM)[a]

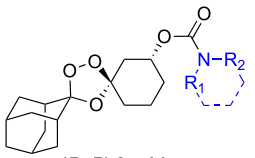

(*R*, *R*) **8a-dd**

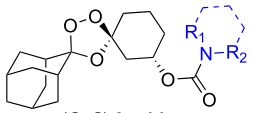

(*S*, *S*) **9a-dd**

8a[1] 1.8 ± 0.1nM
9a[1] 2.1 ± 0.1nM

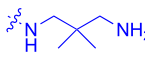

8b[1] 2.9 ± 0.2nM
9b[1] 3.2 ± 0.4nM

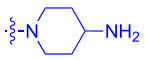

8c[1] 1.7 ± 0.1nM
9c[1] 2.4 ± 0.3nM

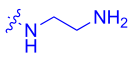

8d[1] 2.8 ± 0.2nM
9d 5.0 ± 2.4nM

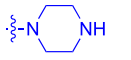

8e[1] 2.2 ± 0.3nM
9e 5.0 ± 0.3nM

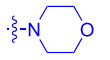

8f[1] 6.8 ± 0.4nM
9f 4.6 ± 1.0nM

8g[1] 60 ± 1.3nM
9g 9.6 ± 1.5nM

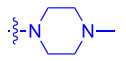

8h[1] 4.4 ± 0.3nM
9h n.d.

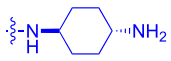

8i[1] 5.8 ± 0.6nM
9i 1.8 ± 0.1nM

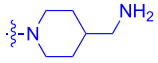

8j[1] 6.8 ± 1.4nM
9j 4.1 ± 1.8nM

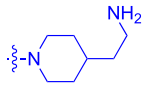

8k[1] 5.0 ± 0.4nM
9k 1.7 ± 1.6nM

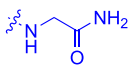

8l[1] 4.9 ± 1.3nM
9l 18.5 ± 11.4nM

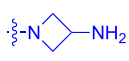

8m[1] 4.6 ± 0.4nM
9m 11.9 ± 5.8nM

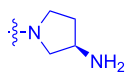

8n[1] 2.4 ± 0.3nM
9n 7.5 ± 5.1nM

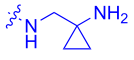

8o 1.5 ± 0.1nM
9o 2.2 ± 0.6nM

8p 0.5 ± 0.2nM
9p 2.0 ± 0.5nM

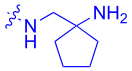

8q 15.0 ± 3.6nM
9q 1.7 ± 0.3nM

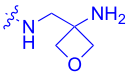

8r 2.7 ± 0.4nM
9r 0.6 ± 0.2nM

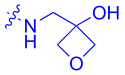

8s 19.3 ± 4.4nM
9s 23.4 ± 3.1nM

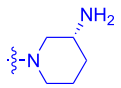

8t 15.0 ± 2.5nM
9t 3.2 ± 1.6nM

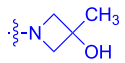

8u 26.4 ± 17.8nM
9u 42.6 ± 48.7nM

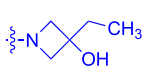

8v 6.3 ± 6.8nM
9v 2.1 ± 1.3nM

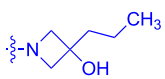

8w 1.1 ± 0.5nM
9w 2.4 ± 2.1nM

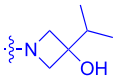

8x 2.4 ± 1.6nM
9x 1.0 ± 0.5nM

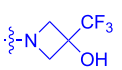

8y 11.7 ± 3.0nM
9y 4.2 ± 2.0nM

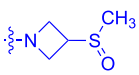

8z 2.6 ± 1.3nM
9z 11.8 ± 5.9nM

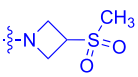

8aa 2.0 ± 0.6nM
9aa 3.3 ± 1.7nM

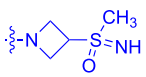

8bb 4.8 ± 3.4nM
9bb 1.9 ± 0.6nM

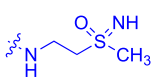

8cc 9.2 ± 19.3nM
9cc 85.9 ± 35.7nM

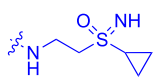

8dd 87.7 ± 56.7nM
9dd 9.1 ± 15.2nM

[a]Reported EC_{50} values are the means of at least three determinations.

Table 1. In Vitro ADME Data for Selected Analogues and Controls

	HLM CL_{int} (μL/min/mg)	Solubility PBS (μM)		HLM CL_{int} (μL/min/mg)	Solubility PBS (μM)		HLM CL_{int} (μL/min/mg)	Solubility PBS (μM)
OZ277	<7[a]	504[b]	**8n**	45.8	167	**9w**	683	18.2
OZ439	63.7[a]	0.181[b]	**9n**	58.7	-	**8v**	480	58.7
8a[a]	12.8	-	**8o**	41.7	-	**9v**	638	41.5
9a[a]	<11.5	174	**9o**	37.4	143	**8x**	392	15.9
8b[a]	14.3	-	**8p**	37.4	142	**9x**	657	15.1
9b[a]	21.4	164	**9p**	24.9	162	**8y**	234	24.8
8c[a]	123	145	**8q**	29.9	162	**9y**	211	10.8
9c[a]	11.8	118	**9q**	25.3	13.4	**8z**	516	138
9d	23.1	144	**8r**	23.4	122	**9z**	750	184
8e[a]	39.4	144	**9r**	135	87.7	**8aa**	526	66.7
9e	120	167	**8s**	76.2	-	**9aa**	851	81.1
9g	<11.6	-	**9s**	333	112	**8bb**	234	268
9h	-	109	**8t**	43.7	74.9	**9bb**	431	142
9i	28.2	-	**9t**	52.7	129	**8cc**	243	128
9j	69.6	112	**8u**	-	71.4	**9cc**	319	129
9k	92.7	117	**9u**	-	137	**8dd**	435	79.3
9m	<11.6	101	**8w**	579	16.1	**9dd**	450	234

[a]data from our preliminary report.[15] [b]data from ref.[20] HLM CL_{int} is human liver microsome intrinsic clearance.

In a recent report on the SAR of antimalarial benzoxaboroles,[19] a dramatic and favorable effect was noted for analogues with azetidine-bearing side chains, in many cases improving in vivo efficacy dramatically. Since the benzoxaborole warhead is known to be essential for antiplasmodial activity in this class and was retained across the analogues studied, we inferred that the improved *in vivo* efficacy of azetidinyl analogues most likely stemmed from improved uptake, reduced efflux, and/or favorable modulation of other ADME properties arising from the azetidine side chains. With a hypothesis that similar

https://doi.org/10.1021/acsmedchemlett.4c00365
ACS Med. Chem. Lett. 2024, 15, 1764−1770

Table 2. Oral Efficacy of *trans*-R^3 Analogues and Controls in *P. berghei*-Infected Female Swiss Webster Mice

Experiment 1		Days[a]	Experiment 3		Days[a]	Experiment 4 (cont.)		Days[a]
OZ439		30	OZ439	1d × 20 mg/kg	30	**9r**		9
8a	1d × 20 mg/kg	12	**8c**	1d × 50 mg/kg	12	**8u**	2d × 10 mg/kg	7
8c		14		2d × 10 mg/kg	30	**8y**		9
				2d × 4 mg/kg	11			
Experiment 2		Days[a]	Experiment 4		Days[a]	Experiment 5		Days[a]
OZ439		30				OZ277		14
9a		10	OZ277		14	**9d**		30
8c		11	**9a**		30	**8q**		11
9c		9	**8c**		12	**8r**		8
9g	1d × 20 mg/kg	7	**9c**	2d × 10 mg/kg	11	**8s**	2d × 10 mg/kg	6
9m		5	**9o**		11	**9s**		6
9o		11	**8p**		13	**8t**		12
8r		7	**9q**		14	**9u**		4
						9dd		6

[a]maximal survival benefit as indicated by days postinfection for longest-surviving mouse in each group (n = 5). Vehicle-treated mice survive 4−5 days postinfection. Mice with no parasitemia at day 30 were judged to be cured. Kaplan−Meier curves are provided for the five experiments as Figure S1 (Supporting Information).

favorable effects might be transferrable to the trioxolane pharmacophore, we synthesized *trans*-3″ carbamates with various alkyl-substituted azetidine alcohols (**8u−y**, **9u−y**) as well as sulfoxide-, sulfone-, and sulfoximine-substituted azetidines (**8z-8bb**, **9z-9bb**), and also two alicyclic sulfoximine analogues (**8cc-8dd**, **9cc-9dd**). Indeed, we observed low-nM antiparasitic activity across all of the substituted azetidine analogues, which notably are neutral, lacking the basic amine functions present in the earlier potent carbamate analogues. By contrast, the alicyclic sulfoximines **8cc/dd** and **9cc/dd**, were less potent overall and showed the largest difference in potency between stereoisomeric pairs.

A majority of the new analogues was evaluated for in vitro human liver microsome (HLM) stability and kinetic solubility in pH 7.4 PBS (Table 2). As expected, the presence of a primary basic amine, or sulfoxide or sulfoximine in the side chain generally resulted in high kinetic solubilities in excess of 100 μM. With regard to HLM stability, we previously observed excellent clearance values for the enantiomer pairs **8a**/**9a** and **8b**/**9b**, whereas **8c** was much more rapidly metabolized than **9c**, which showed HLM clearance (CL) values similar to **8a**/**9a**/**8b**/**9b**. Additional enantiomer pairs evaluated here included the full set of **8n-dd**/**9n-dd** (Table 2). The amine-bearing enantiomer pairs **8n−r**/**9n−r** showed moderate to high clearance, with only **8r**/**9r** showing a significant stereoisomer effect. The lowest clearance values of the new carbamate analogues were for **9g** (piperidinyl) and **9m** (aminoazetidinyl), both of which had HLM CL < 11.6 μL/min/mg. Unfortunately, and despite their potent antiparasitic effects, the large subset of substituted azetidinyl carbamates **8u-bb** and **9u-bb** was very rapidly metabolized in the HLM preparations, suggesting a particular metabolic liability of this ring system in the context of the trioxolane 3″-carbamate chemotype. Similarly, the alicyclic sulfoximine analogues **8cc/dd** and **9cc/dd** also exhibited rapid HLM clearance.

Next, we used the *P. berghei* mouse model of malaria to assess the oral efficacy of selected new carbamate analogues, using arterolane (OZ277) or artefenomel (OZ439) as positive controls (Table 2). Briefly, female Swiss-Webster mice were infected intraperitoneally with *P. berghei*-infected murine erythrocytes, following which mice were treated via oral gavage with 100 μL of formulated test compound or vehicle according to the dosing paradigm indicated (Table 2). Cohorts were organized with five animals per treatment group, Giemsa-stained blood smears were taken over time to monitor parasitemia, and animals were considered cured if parasitemia could not be detected at day 30. All regimens were well-tolerated, with no overt signs of toxicity for any of the analogues studied.

In our previous report, we explored both repeat and single-exposure regimens, finding that the most efficacious carbamates could afford cures in some animals with a single 40 mg/kg dose. For comparison, artefenomel was reported[8] to produce cures at half this dose. Since artefenomel represents a benchmark for single-exposure efficacy in the *P. berghei* model, we chose to evaluate new carbamates at a single 20 mg/kg dose, comparing survival benefits to those afforded by artefenomel at the same dose. In the first in vivo experiment conducted using this 1 × 20 mg/kg protocol, we found that previously described analogues **8a** and **8c** extended survival up to 12 and 14 days, respectively, compared to 5 days for vehicle control, and 30 days for artefenomel (Table 2 Supplemental Figure S1). A half-dozen new analogues evaluated in experiment 2 showed less significant survival benefits, although **9o** was as effective as **8c**, the latter among the best analogues from the original study.

We next explored various two-dose regimens that we expected should show a broader range of survival benefit and thereby allow more meaningful rank-odering of new analogues. Using analogue **8c** as test article for a dose-ranging study, we compared regimens of 10 mg/kg once daily for 2 days (producing 3/5 cures at day 30) and 4 mg/kg once daily for 2 days (survival benefit to 11 days, but no cures). This experiment thus nominated the 10 mg/kg × 2d regimen as a new benchmark for studying the efficacy of carbamate analogues.

Using the new once daily for 2 days regimen, we found in experiment 4 that **9a** produced cures in 3/5 mice, consistent with the favorable efficacy of its enantiomer **8a** in our previous report. It was interesting that **8c** (also included in experiment 4) produced no cures, in contrast to the 3/5 cures produced in experiment 3. We attribute this to biological variation and the possibility that animals in experiment 4 received a larger inoculum. In any event, the superior efficacy of **9a** vs **8c** in

https://doi.org/10.1021/acsmedchemlett.4c00365
ACS Med. Chem. Lett. 2024, 15, 1764−1770

experiment 4 was gratifying. Of the remaining analogues explored in experiment 4, none produced cures, although structurally similar analogues **9q** and **8p** exhibited the most favorable effects on survival, with end points extended to 14 and 13 days, respectively (Supplemental Figure S1)

In experiment 5, we evaluated eight additional analogues, and were excited to find that (*S,S*) enantiomer **9d**, an analogue of **9a** lacking the gem-dimethyl side-chain substitution, produced cures in all five mice and thus represents the most efficacious analogue identified in the current study (Figure S1, Supporting Information). In stark contrast, analogues **8r**, **8s**, **9s**, **9u**, and **9dd** performed poorly, providing little additional benefit over vehicle treated animals. Thus, the 10 mg/kg × 2d regimen readily distinguished analogues with curative efficacy such as **9a** and **9d** from those exhibiting more modest survival benefit (e.g., **8c**, **8p**, **9q**) and further, from those with little to no efficacy (**8r**−**s**, **9s**, **9u**).

In a final in vivo study (experiment 6, Figure 3), we compared **9a** with analogue **9p** (enantiomer of analogue **8p**),

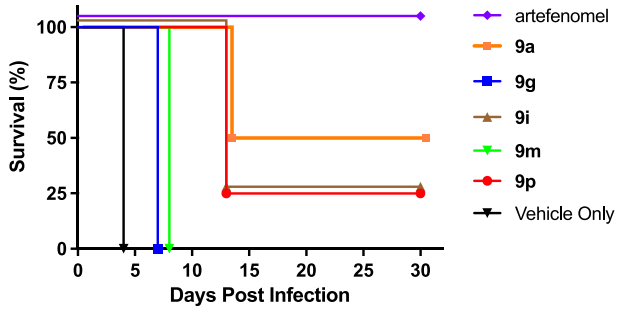

Figure 3. Results of in vivo experiment 6, showing the survival of mice treated with test compound or artefenomel control with 2 × 10 mg/kg oral doses. Mice surviving at day 30 were judged to be cured.

and three carbamates bearing different cyclic ring systems—the piperidine **9g**, aminoazetidine **9m**, and 1,4-diaminocyclohexane **9i**. The results of this study largely confirmed the emerging structure-efficacy trends for the series. Thus, analogue **9p** (13 days survival and 1 cure) showed efficacy that was very similar to that of its enantiomer **8p**. The analogue **9i**, bearing a terminal primary amine, also performed well, and identically to **9p**. The least efficacious analogue was piperidine **9g**, which lacks the basic amine function found in most of the efficacious analogues. Most disappointing in this light was the aminoazetidine **9m**, which despite bearing basic amine functionality and showing potent in vitro activity, performed only marginally better than **9g** and the vehicle control.

In our earlier report[15] on *trans*-3″ carbamates, we identified **8a**, **8c**, and **8d** as the most promising with respect to in vivo efficacy, all three proving superior to arterolane in terms of cures, following a 2 mg/kg × 4d regimen. In terms of reduced frequency dosing, compound **8c** was most extensively studied and notably produced cures (8/10 animals in two separate studies) with a single 40 mg/kg dose. To these leads we can now add (*S,S*) analogues **9a**, **9d**, **9i**, and **9p** as additional examples of this chemotype exhibiting promising in vivo efficacy with reduced dosing frequencies.

To better understand PK/PD relationships in this chemotype, we performed mouse PK studies of **8a**, **9a**, and **9d** with oral and IV administration at 10 and 3 mg/kg, respectively (Table 3 and Table S1). We found that (*S,S*) analogue **9a** showed reduced clearance and ∼50% higher AUC than its (*R,R*) enantiomer **8a**, while the volume of distribution and bioavailability were similar at ∼2.5 L/kg and ∼39%, respectively (Table 3). Analogue **9d** exhibited lower clearance than either **8a** or **9a**, the highest AUC, and similar volumes of distribution and oral bioavailability. The reported[7] half-life (1.4 h) and bioavailability (35%) of arterolane in rat is thus comparable to that for **8a**/**9a**/**9d** in mouse. Consistent with the superior efficacy of **9d** over arterolane in our studies, it was previously reported[7] that *three* daily 10 mg/kg doses of arterolane produced a 67% cure rate in the *P. berghei* model. This compares with the fully curative efficacy achieved herein with just two 10 mg/kg daily oral doses of **9d** (experiments 4 and 5, Table 1 and Figure S1).

Herein we described the stereocontrolled synthesis and in vitro and in vivo evaluation of novel *trans*-3″ substituted 1,2,4-trioxolane carbamates, focusing on analogues with small to medium-size rings and bearing primary amine, alcohol, or sulfinyl functionality. We found that acyclic, primary amine-bearing carbamates exhibited the most promising efficacy in a murine malaria model and also the best metabolic stability in human liver microsomes. Exemplar *trans*-3″ carbamate **9d** produced complete cures in the *P. berghei* model after two daily 10 mg/kg oral doses, demonstrating efficacy superiority to arterolane under this regimen and equivalent to artefenomel at 1 day × 20 mg/kg. Although some improvements over arterolane in PK and PD profiles can be realized in *trans*-3″ carbamates like **8a**/**9a**/**9d**, their PK profiles are more similar to those of arterolane than artefenomel. Accordingly, we judge that a single-exposure cure may be an unrealistic objective for this chemotype. On the other hand, **9d** exhibited efficacy equivalent to 20 mg/kg × 1d artefenomel under the 10 mg/kg × 2d regimen, while exhibiting superior HLM stability and dramatically improved solubility. While useful for in vivo screening, the *P. berghei* model is limited in its ability to predict efficacy and dose to treat human malaria. The humanized SCID mouse model of *P. falciparum*[21] represents the current preclinical benchmark for evaluating the efficacies of antimalarial drug candidates. The *trans*-3″ chemotype and optimized analogues such as **9d** identified here are promising leads appropriate for evaluation in this model and as leads for the discovery of next generation antimalarial trioxolanes.

Table 3. In Vitro Human Microsome Clearance and Selected PK Parameters for Compounds 8a, 9a, and 9d

	in vitro ADME	in vivo PK (IV dose 3 mg/kg)		in vivo PK (PO dose 10 mg/kg)		
compound	HLM (μL/min/mg)	CL (L/h/kg)	Vss (L/kg)	$T_{1/2}$ (hr)	AUC_{last} (ng/mL*hr)	*F* (%)
8a	12.8	6.51	2.79	2.09	555	39.3
9a	<11.5	4.62	2.50	1.44	818	38.9
9d	23.1	3.96	2.33	1.66	1038	43.1

https://doi.org/10.1021/acsmedchemlett.4c00365
ACS Med. Chem. Lett. 2024, 15, 1764−1770

EXPERIMENTAL PROCEDURES

EC_{50} of Experimental Compounds against Cultured *P. falciparum* Parasites. Caution! *P. falciparum* is a Biosafety Level-2 (BSL-2) human pathogen and was handled by using BSL-2 procedures. Erythrocytic cultures of *P. falciparum* strain W2 (BEI Resources) were maintained using standard methods at 2% hematocrit in RPMI 1640 medium (Invitrogen) supplemented with 0.5% AlbuMAX II (Gibco Life Technologies), 0.1 mM hypoxanthine, 30 μg/mL gentamicin, 24 mM $NaHCO_3$, and 25 mM HEPES pH 7.4 at 37 °C in an atmosphere of 5% O_2, 5% CO_2, and 90% N_2. Infected cultures were exposed to 12 drug concentrations (3-fold serial dilution from 10 μM −0.06 nM) or an equal volume of DMSO with tips changed between each serial dilution to minimize potential carryover of lipophilic compounds. Test plates were incubated at 37 °C under the above atmosphere for 72 h, following which erythrocytes were pelleted and fixed in 2% formaldehyde in PBS (pH 7.4) at room temperature overnight. 2% Formaldehyde PBS was removed, and parasites were resuspended in permeabilization media (100 mM NH_4Cl, 0.1% Triton-X, PBS pH 7.4) with freshly added 25 nM YOYO-1 fluorescent dye. Plates were incubated at 4 °C for a minimum of 24 h. Parasitemia was determined from dot plots of 5×10^4 cells acquired on a FACSCalibur flow cytometer using CELLQUEST software (Becton Dickinson), using initial gating values determined from unstained uninfected erythrocyte and stained uninfected erythrocyte controls. IC_{50}s were determined using GraphPad Prism software with 3 experimental replicates per compound.

***P. berghei* Mouse Malaria Model.** Female Swiss Webster mice (~20 g body weight) were infected intraperitoneally with 10^6 *P. berghei*-infected erythrocytes collected from a previously infected mouse. Beginning 1 h after inoculation, the mice were treated once daily by oral gavage for 1−2 days as indicated with 100 μL of solution of test compound formulated in 10% DMSO: 50% PEG400:40% of a 20% HP-β-CD solution in water. There were five mice in each test arm. Infections were monitored by daily microscopic evaluation of Giemsa-stained blood smears starting on day seven. Parasitemia was determined by counting the number of infected erythrocytes per 1000 erythrocytes. Body weight was measured over the course of the treatment. Mice were euthanized when parasitemia exceeded 50% or when a weight loss of more than 15% occurred. Parasitemia, animal survival, and morbidity were closely monitored for 30 days postinfection, when experiments were terminated.

Pharmacokinetic Studies. Pharmacokinetic studies with IV (3 mg/kg) and PO (10 mg/kg) dosing was performed in male CD1 mice (n = 3 per group) with a formulation 10% DMSO: 50% PEG400:40% of a 20% HP-β-CD solution in water. Microsampling (40 mL) via facial vein was performed at 0, 0.083, 0.25, 0.5, 1, 2, 4, 8, and 24 h into K_2EDTA tubes. The blood samples were collected and centrifuged to obtain plasma (8000 rpm, 5 min) within 15 min post sampling. Nine blood samples were collected from each mouse; three samples were collected for each time point. Data was processed by Phoenix WinNonlin (version 8.3); samples below limit of quantitation were excluded in the PK parameters and mean concentration calculation.

Animal Welfare. No alternative to the use of laboratory animals is available for in vivo efficacy assessments. Animals were housed and fed according to NIH and USDA regulations in the Animal Care Facility at San Francisco General Hospital. Trained animal care technicians provide routine care, and veterinary staff is readily available. Euthanasia was performed when malaria parasitemias topped 50%, a level that does not appear to be accompanied by distress but predicts progression to lethal disease. Euthanasia was accomplished with CO_2 followed by cervical dislocation. These methods are in accordance with the recommendations of the Panel on Euthanasia of the American Veterinary Medical Association. Our studies have been approved by the UCSF Committee on Animal Research.

ASSOCIATED CONTENT

Supporting Information

The Supporting Information is available free of charge at https://pubs.acs.org/doi/10.1021/acsmedchemlett.4c00365.

Kaplan−Meier survival curves, pharmacokinetic parameters, synthetic procedures (PDF)

AUTHOR INFORMATION

Corresponding Author

Adam R. Renslo − *Department of Pharmaceutical Chemistry, University of California, San Francisco, San Francisco, California 94158, United States;* orcid.org/0000-0002-1240-2846; Phone: 415-514-9698; Email: adam.renslo@ucsf.edu; Fax: 415-514-4507

Authors

Matthew T. Klope − *Department of Pharmaceutical Chemistry, University of California, San Francisco, San Francisco, California 94158, United States*

Juan A. Tapia Cardona − *Department of Pharmaceutical Chemistry, University of California, San Francisco, San Francisco, California 94158, United States; Department of Medicine, San Francisco General Hospital, University of California, San Francisco, California 94143, United States*

Jun Chen − *Department of Pharmaceutical Chemistry, University of California, San Francisco, San Francisco, California 94158, United States*

Ryan L. Gonciarz − *Department of Pharmaceutical Chemistry, University of California, San Francisco, San Francisco, California 94158, United States*

Ke Cheng − *Department of Pharmaceutical Chemistry, University of California, San Francisco, San Francisco, California 94158, United States;* orcid.org/0000-0001-5057-3120

Priyadarshini Jaishankar − *Department of Pharmaceutical Chemistry, University of California, San Francisco, San Francisco, California 94158, United States*

Julie Kim − *Department of Pharmaceutical Chemistry, University of California, San Francisco, San Francisco, California 94158, United States*

Jenny Legac − *Department of Medicine, San Francisco General Hospital, University of California, San Francisco, California 94143, United States*

Philip J. Rosenthal − *Department of Medicine, San Francisco General Hospital, University of California, San Francisco, California 94143, United States*

Complete contact information is available at: https://pubs.acs.org/10.1021/acsmedchemlett.4c00365

Author Contributions

M.K., P.J.R., and A.R.R. conceived of experiments. M.K, J.C., R.L.G, K.C., P.J., and J.K. synthesized compounds. M.K, J.A.T., and J.L performed in vitro antiplasmodial assays and the mouse infection model. M.K. and A.R.R. drafted the manuscript and all authors reviewed and/or edited the manuscript.

Notes

The authors declare the following competing financial interest(s): A.R.R. holds equity in Tatara Therapeutics, Inc. which seeks to develop iron-activated therapeutics for cancer and infectious disease.

https://doi.org/10.1021/acsmedchemlett.4c00365
ACS Med. Chem. Lett. 2024, 15, 1764−1770

■ ACKNOWLEDGMENTS

A.R.R. acknowledges funding from the US National Institutes of Health, R01 Grant AI105106.

■ ABBREVIATIONS

(ART-R), artemisinin partial resistance; (PK), pharmacokinetic; (PD), pharmacodynamic; (HLM), human liver microsome; (ADME), absorption, distribution, metabolism and excretion

■ REFERENCES

(1) World Health Organization (WHO).*World Malaria Report 2023*; WHO: Geneva, 2023.
(2) Conrad, M. D.; Asua, V.; Garg, S.; Giesbrecht, D.; Niaré, K.; Smith, S.; Namuganga, J. F.; Katairo, T.; Legac, J.; Crudale, R. M.; Tumwebaze, P. K.; Nsobya, S. L.; Cooper, R. A.; Kamya, M. R.; Dorsey, G.; Bailey, J. A.; Rosenthal, P. J. Evolution of Partial Resistance to Artemisinins in Malaria Parasites in Uganda. *N. Engl. J. Med.* **2023**, *389*, 722−732.
(3) Rosenthal, P. J.; Asua, V.; Conrad, M. D. Emergence, transmission dynamics and mechanisms of artemisinin partial resistance in malaria parasites in Africa. *Nat. Rev. Microbiol.* **2024**, *22*, 373−384.
(4) Woodley, C. M.; Amado, P. S. M.; Cristiano, M. L. S.; O'Neill, P. M. Artemisinin Inspired Synthetic Endoperoxide Drug Candidates: Design, Synthesis, and Mechanism of Action Studies. *Med. Res. Rev.* **2021**, *41*, 3062−3095.
(5) Dong, Y.; Wittlin, S.; Sriraghavan, K.; Chollet, J.; Charman, S. A.; Charman, W. N.; Scheurer, C.; Urwyler, H.; Santo Tomas, J.; Snyder, C.; Creek, D. J.; Morizzi, J.; Koltun, M.; Matile, H.; Wang, X.; Padmanilayam, M.; Tang, Y.; Dorn, A.; Brun, R.; Vennerstrom, J. L. The Structure-Activity Relationship of the Antimalarial Ozonide Arterolane (OZ277). *J. Med. Chem.* **2010**, *53*, 481−491.
(6) Dong, Y.; Wang, X.; Kamaraj, S.; Bulbule, V. J.; Chiu, F. C. K.; Chollet, J.; Dhanasekaran, M.; Hein, C. D.; Papastogiannidis, P.; Morizzi, J.; Shackleford, D. M.; Barker, H.; Ryan, E.; Scheurer, C.; Tang, Y.; Zhao, Q.; Zhou, L.; White, K. L.; Urwyler, H.; Charman, W. N.; Matile, H.; Wittlin, S.; Charman, S. A.; Vennerstrom, J. L. Structure-Activity Relationship of the Antimalarial Ozonide Artefenomel (OZ439). *J. Med. Chem.* **2017**, *60*, 2654−2668.
(7) Vennerstrom, J. L.; Arbe-Barnes, S.; Brun, R.; Charman, S. A.; Chiu, F. C. K.; Chollet, J.; Dong, Y.; Dorn, A.; Hunziker, D.; Matile, H.; McIntosh, K.; Padmanilayam, M.; Santo Tomas, J.; Scheurer, C.; Scorneaux, B.; Tang, Y.; Urwyler, H.; Wittlin, S.; Charman, W. N. Identification of an Antimalarial Synthetic Trioxolane Drug Development Candidate. *Nature* **2004**, *430*, 900−904.
(8) Charman, S. A.; Arbe-Barnes, S.; Bathurst, I. C.; Brun, R.; Campbell, M.; Charman, W. N.; Chiu, F. C. K.; Chollet, J.; Craft, J. C.; Creek, D. J.; Dong, Y.; Matile, H.; Maurer, M.; Morizzi, J.; Nguyen, T.; Papastogiannidis, P.; Scheurer, C.; Shackleford, D. M.; Sriraghavan, K.; Stinge-lin, L.; Tang, Y.; Urwyler, H.; Wang, X.; White, K. L.; Wittlin, S.; Zhou, L.; Vennerstrom, J. L. Synthetic Ozonide Drug Candidate OZ439 Offers New Hope for a Single-Dose Cure of Uncomplicated Malaria. *Proc. Natl. Acad. Sci. U. S. A.* **2011**, *108*, 4400−4405.
(9) Straimer, J.; Gnädig, N. F.; Stokes, B. H.; Ehrenberger, M.; Crane, A. A.; Fidock, D. A. Plasmodium Falciparum K13 Mutations Differentially Impact Ozonide Susceptibility and Parasite Fitness In Vitro. *MBio* **2017**, *8*, e00172-17.
(10) Giannangelo, C.; Fowkes, F. J. I.; Simpson, J. A.; Charman, S. A.; Creek, D. J. Ozonide Antimalarial Activity in the Context of Artemisinin-Resistant Malaria. *Trends Parasitol.* **2019**, *35*, 529−543.
(11) Kim, H. S.; Hammill, J. T.; Guy, R. K. Seeking the Elusive Long-Acting Ozonide: Discovery of Artefenomel (OZ439). *J. Med. Chem.* **2017**, *60*, 2651−2653.
(12) White, N. J.; Nosten, F. H. SERCAP: Is the Perfect the Enemy of the Good? *Malar. J.* **2021**, *20*, 281.
(13) Salim, M.; Khan, J.; Ramirez, G.; Clulow, A. J.; Hawley, A.; Ramachandruni, H.; Boyd, B. J. Interactions of Artefenomel (OZ439) with Milk during Digestion: Insights into Digestion-Driven Solubilization and Polymorphic Transformations. *Mol. Pharmaceutics* **2018**, *15*, 3535−3544.
(14) Clulow, A. J.; Salim, M.; Hawley, A.; Gilbert, E. P.; Boyd, B. J. The Curious Case of the OZ439 Mesylate Salt: An Amphiphilic Antimalarial Drug with Diverse Solution and Solid State Structures. *Mol. Pharmaceutics* **2018**, *15*, 2027−2035.
(15) Blank, B. R.; Gonciarz, R. L.; Talukder, P.; Gut, J.; Legac, J.; Rosenthal, P. J.; Renslo, A. R. Antimalarial Trioxolanes with Superior Drug-Like Properties and In Vivo Efficacy. *ACS Infect. Dis.* **2020**, *6*, 1827−1835.
(16) Blank, B. R.; Gut, J.; Rosenthal, P. J.; Renslo, A. R. Enantioselective Synthesis and in Vivo Evaluation of Regioisomeric Analogues of the Antimalarial Arterolane. *J. Med. Chem.* **2017**, *60*, 6400−6407.
(17) Blank, B. R.; Gut, J.; Rosenthal, P. J.; Renslo, A. R. Artefenomel Regioisomer RLA-3107 Is a Promising Lead for the Discovery of Next-Generation Endoperoxide Antimalarials. *ACS Med. Chem. Lett.* **2023**, *14*, 493−498.
(18) Woodley, C. M.; Nixon, G. L.; Basilico, N.; Parapini, S.; Hong, W. D.; Ward, S. A.; Biagini, G. A.; Leung, S. C.; Taramelli, D.; Onuma, K.; Hasebe, T.; O'Neill, P. M. Enantioselective Synthesis and Profiling of Potent, Nonlinear Analogues of Antimalarial Tetraoxanes E209 and N205. *ACS Med. Chem. Lett.* **2021**, *12*, 1077−1085.
(19) Zhang, Y.-K.; Plattner, J. J.; Easom, E. E.; Jacobs, R. T.; Guo, D.; Freund, Y. R.; Berry, P.; Ciaravino, V.; Erve, J. C. L.; Rosenthal, P. J.; Campo, B.; Gamo, F.-J.; Sanz, L. M.; Cao, J. Ben-zoxaborole Antimalarial Agents. Part 5. Lead Optimization of Novel Amide Pyrazinyloxy Benzox-aboroles and Identification of a Preclinical Candidate. *J. Med. Chem.* **2017**, *60*, 5889−5908.
(20) Charman, S. A.; Andreu, A.; Barker, H.; Blundell, S.; Campbell, A.; Campbell, M.; Chen, G.; Chiu, F. C. K.; Crighton, E.; Katneni, K.; Morizzi, J.; Patil, R.; Pham, T.; Ryan, E.; Saunders, J.; Shackleford, D. M.; White, K. L.; Almond, L.; Dickins, M.; Smith, D. A.; Moehrle, J. J.; Burrows, J. N.; Abla, N. An in Vitro Toolbox to Accelerate Anti-Malarial Drug Discovery and Development. *Malar. J.* **2020**, *19*, 1.
(21) Jiménez-Díaz, M. B.; Mulet, T.; Viera, S.; Gómez, V.; Garuti, H.; Ibáñez, J.; Alvarez-Doval, A.; Shultz, L. D.; Martínez, A.; Gargallo-Viola, D.; Angulo-Barturen, I. Improved Murine Model of Malaria Using Plasmodium Falciparum Competent Strains and Non-Myelodepleted NOD-Scid IL2Rgammanull Mice Engrafted with Human Erythrocytes. *Antimicrob. Agents Chemother.* **2009**, *53*, 4533−4536.

https://doi.org/10.1021/acsmedchemlett.4c00365
ACS Med. Chem. Lett. 2024, 15, 1764−1770